Journal of Molecular Structure 993 (2011) 495–499

Contents lists available at ScienceDirect

Journal of Molecular Structure

journal homepage: www.elsevier.com/locate/molstruc

Laser sources for efficient two-step Positronium excitation to Rydberg states

M. Becucci [a,b,*], G. Ferrari [a,c,d], I. Boscolo [e,f], F. Castelli [e,f], S. Cialdi [e,f], F. Villa [e,f], M.G. Giammarchi [f]

[a] LENS-Università di Firenze, via Carrara 1, 50019 Sesto Fiorentino, Italy
[b] Dipartimento di Chimicà Ugo Schiff-Università di Firenze, via della Lastruccia 3, 50019 Sesto Fiorentino, Italy
[c] INO-CNR BEC Center, via Sommarive 14, 38123 Povo, Italy
[d] INFN-Sezione di Firenze, via Carrara 1, 50019 Sesto Fiorentino, Italy
[e] Università degli Studi di Milano, via Celoria 16, 20133 Milano, Italy
[f] Istituto Nazionale di Fisica Nucleare, sezione di Milano, via Celoria 16, 20133 Milano, Italy

ARTICLE INFO

Article history:
Available online 5 March 2011

Keywords:
Positronium
Rydberg states
Zeeman and Stark effects
Antihydrogen

ABSTRACT

Antihydrogen production by charge exchange reaction between Positronium atoms and antiprotons benefits from an efficient excitation of Positronium atoms to high-n levels (Rydberg levels). A two-step optical excitation, the first from ground to $n = 3$ and the second from this level to a Rydberg level, is proposed and a proper laser system to be developed is discussed. The requirements on the energy and bandwidth of the excitation laser suggest the use of optical parametric generation technology for both wavelengths. The laser system is composed of two subsystems: one for the generation of 205 nm radiation and the other for the generation of 1670 nm radiation. We report on the progress towards the realization of the short wavelength source.

1. Introduction

Efficient Positronium (Ps) excitation to high-n levels is pursued in some experiments on antihydrogen $\overline{H}$ generation. In the AEGIS (Antimatter Experiment: Gravity, Interferometry, Spectroscopy) experiment [1–3] the production of cold $\overline{H}$ bunches in highly excited states (Rydberg states) would occur by charge transfer of a cloud of Rydberg-excited Ps atoms with a bunch of cold antiprotons $\bar{p}$ by means of the reaction $Ps^* + \bar{p} \rightarrow \overline{H}^* + e^-$ [4–6].

The efficiency of the antihydrogen production is proportional to the cross section of the charge exchange reaction, which is a function of the fourth power of the principal quantum number n of the excited Ps [4–6] ($\sigma \propto n^4 \pi a_0^2$, where a_0 is the Bohr radius). Choosing n in the range from 20 to 30, as in the AEGIS proposal, increases substantially the recombination efficiency without inducing losses due to ionization.

Positronium excitation to these high-n levels can be obtained either via collisions or via photon-excitation. In Refs. [4–6] Ps excitation was proposed and tested through Cs excitation by light and a successive charge exchange reaction with positrons. In that experiment the production of antihydrogen was essentially a continuous process, while the proposed testing of gravity acceleration in AEGIS needs pulsed beams, both of positrons and antihydrogen, for better time of flight measurements. In the AEGIS experimental program we proposed a direct Ps excitation by a two-step light excitation using two simultaneous nanosecond laser pulses with different wavelengths [1]. The theory of Ps photon-excitation in AEGIS is presented in Ref. [7].

In AEGIS Ps atoms are efficiently produced at a porous silica surface by hitting the silica sheet with a positron bunch at kinetic energies ranging from several 100 eV to a few keV [8,9]. Ps atoms leaving the target surface form an expanding cloud with an initial transverse area of the order of 1 mm diameter, at an effective temperature of the order of 100 K which corresponds to a velocity $v \sim 3 \times 10^4$ m/s RMS. The atoms move in a relatively strong magnetic field $\vec{B}$ of about one Tesla [1]. In these conditions the combination of the Doppler, motional Stark, linear and quadratic Zeeman effects [7,10,11] results in a broadening of the excitation transition frequencies of the order of 1 THz, making the excitation process substantially less selective than in the usual case of Rydberg spectroscopy. This is one of the challenges that the laser system in AEGIS has to face. The characteristics of laser pulses in terms of power and spectral bandwidth must be tailored to the geometry, the level-bandwidths and the timing of the Ps expanding cloud in order to maximize the excitation efficiency of the whole Ps cloud within few nanoseconds.

The photo-excitation of Ps to high-n state requires photon wavelengths close to 182 nm. Since the generation of such a wavelength is not a simple task, we have considered excitation via a two-step optical transition, by exploiting two possible alternatives: the path by the transitions $1 \rightarrow 2$ and $2 \rightarrow$ high-n, and the path with the transitions $1 \rightarrow 3$ and $3 \rightarrow$ high-n. Even if the $1 \rightarrow 2$ transition is well known [12,13] and the two photon-excitation via $1 \rightarrow 2 \rightarrow$ high-n was tested in [14], we have selected the $1 \rightarrow 3 \rightarrow$ high-n excitation

* Corresponding author at: LENS-Università di Firenze, via Carrara 1, 50019 Sesto Fiorentino, Italy.
E-mail address: maurizio.becucci@unifi.it (M. Becucci).

0022-2860/$ - see front matter © 2011 Elsevier B.V. All rights reserved.
doi:10.1016/j.molstruc.2011.01.064

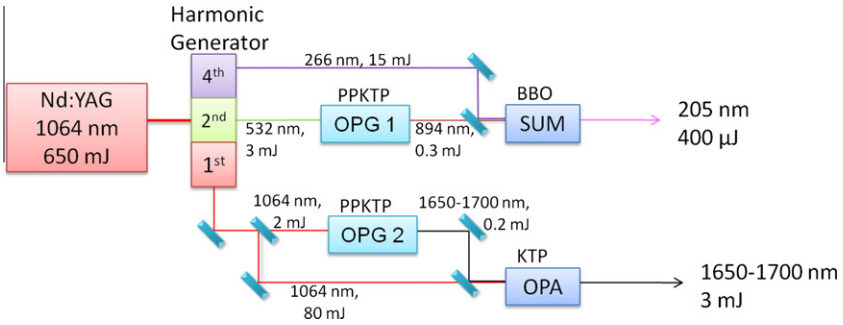

Fig. 1. Laser system for the excitation of Positronium towards Rydberg states.

path for the following considerations [7]: (i) the level $n = 2$ has a lifetime of 3 ns, shorter than the 10.5 ns of the level $n = 3$, (ii) the simulated excitation efficiency is greater in the $1 \rightarrow 3 \rightarrow$ high-n transitions, (iii) the required laser energy per pulse is on the whole lower in the second sequence than the in the first one. The longer lifetime is less demanding with respect to the time-jitter between the two laser pulses, the higher excitation efficiency allows to have more antihydrogen atoms after charge-exchange reaction and lower laser energies are useful in order to maintain easily the low temperature of the cryogenic environment.

Our laser system is based on a Q-switched Nd:YAG producing ~5 ns pulses used to pump nonlinear crystals for parametric generation of the desired wavelengths having a broad, continuum spectrum in order to cover efficiently the Ps Rydberg levels band, as discussed in the following section. With this scheme of two-step incoherent excitation to Rydberg levels an efficiency up to 30% is expected [7]. Other excitation systems can be envisaged in order to obtain better population transfer efficiencies, like π pulses or adiabatic passage techniques [15,16]. These schemes require carefully prepared chirped or transform limited laser pulses. Because Ps excitation in our experiment needs laser pulses with a very broad linewidth and a time duration not longer than a few nanoseconds, required to excite the population more rapidly than the Ps ground state decay by annihilation and the constraint due to the Ps ballistic expansion, these schemes are of difficult implementation in our case. The wavelength range for the radiation used in this experiment (205 nm) is quite of interest for different applications in the field of molecular spectroscopy and reaction dynamics. Therefore the possibilities explored here in terms of spectral range of emission and control of the laser bandwidth could be of interest for different research fields.

2. Scheme of the laser system for Ps excitation

The wavelengths of the two lasers are respectively $\lambda = 205$ nm for the excitation from the ground to $n = 3$ state, and λ in the range from 1650 to 1700 nm for the in-cascade transition. The two lasers have to generate the wide spectral bandwidth $\Delta\lambda_L$ matching the quasi-continuum level-bandwidths of the two Ps transitions. The bandwidths are so wide, especially that required for the second transition, that standard lasers based on optical cavities embodying the laser material are not suited for our Ps excitation. In fact, these lasers operate at definite longitudinal modes giving relatively narrow width lines inside the spectrum envelope. This reduces the excitation efficiency because the wide Ps resonance is not full covered by the comb-like shape of the spectrum.

The laser technology suitable to produce a wide continuum spectrum necessary for efficient excitation as in our case is that based on the optical parametric generation and amplification [17]. We consider the laser system depicted in Fig. 1.

Both radiations are generated through the second-order polarization in optical crystals. The 205 nm radiation is obtained by summing up in a nonlinear BBO crystal the 266 nm fourth-harmonic of the 1064 nm Nd:YAG radiation and the 894 nm radiation generated in an OPG (optical parametric generator) by down-conversion of the 532 nm second-harmonic of the Nd:YAG radiation. The other wavelength is generated in a single step by an OPG and then amplified by an OPA (optical parametric amplifier).

Experimentally, a Q-switched Nd:YAG laser delivering a maximum of 650 mJ in 4 ns drives both laser systems. About half the energy of the Nd:YAG laser is conveyed along the first system (the upper part of Fig. 1), where it is frequency doubled to 532 nm for pumping the first OPG and a second BBO frequency doubling crystal. The remainder of the 1064 nm radiation pumps both the second OPG (a small fraction) and the OPA.

The proposed laser system provides spectral bandwidths large enough to cover the Ps level broadenings as well as the power levels to meet the requirements as discussed in [7]. The laser of the second transition has in addition the capability to operate at frequencies within ~30 nm around the 1670 nm. This allows the selection of the final Ps excited energy (starting from $n = 20$ up to the ionization limit) and gives margin for possible unexpected problems in the excitation. The pulse duration cannot exceed a few nanoseconds in order to be consistent with the Ps flight time from the silica slab to the $\bar{p}$ cloud and to minimize losses due to enhanced annihilation after spontaneous decay to the ground state due to sublevel magnetic mixing.

The pulse energies and spectral bandwidth can satisfy the requirements for maximization of the Ps transition efficiency, with the goal to generate pulses with an energy about 10 times higher than required. This will allow to compensate for the losses expected on the line to bring the light to the PS formation region and, more generally, will provide a safety margin for the PS excitation.

3. The 205 nm laser system design

The laser system at 205 nm responsible for the excitation ($n = 1 \rightarrow n = 3$) has the following requirements:

1. spectral bandwidth larger than 30 GHz RMS, mainly to account for the Doppler broadening,
2. an almost continuous spectrum (*i.e.* without the comb-like structure typically due to the mode spacing of an optical cavity),
3. a pulse duration shorter than 10 ns,
4. an integrated energy many times larger than 2.2 μJ.

These requirements on the wavelength and the energy per pulse are not as trivial to fulfill. Producing 205 nm photons by direct parametric down-conversion is not realistic because of the lack of suitable pump lasers at wavelengths shorter than 205 nm, while approaches based on harmonic generation, such as frequency doubling or tripling, on down-converted photons at

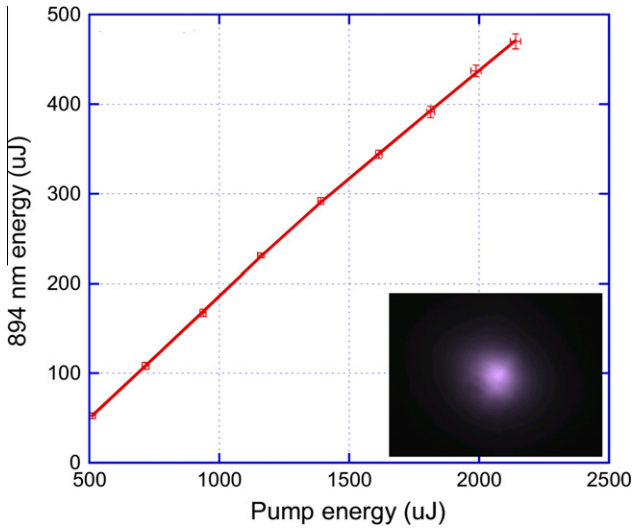

Fig. 2. Power generated at 895 nm with a PPKTP-baser optical parametric generator (OPG) pumped by the 532 nm Q-switched laser. Inset: Beam profile of the radiation generated at 895 nm.

longer wavelength are not viable mainly because of the limited efficiency reachable in the harmonic process. Other approaches based on harmonic generation of a longer wavelength laser, such as tripling of 615 nm suggested in [6] and proposed in a former Ps excitation scheme [3], may turn out to be challenging to implement.

Given this, we will consider a different approach based both on parametric down-conversion and frequency summing processes [18]. Here the requirements 1 and 2 are satisfied by generating radiation at 894 nm with an OPG pumped by a nanosecond laser at 532 nm. Subsequently the 894 nm light is frequency summed to the second-harmonic of the same pump laser, at a wavelength of 266 nm, hence generating 205 nm radiation. Compared to the case of direct harmonic generation of the OPG-generated radiation, with our approach the conversion process towards 205 nm is considerably more effective because of the large amount of energy available at 266 nm with nanosecond lasers, which boosts the nonlinear conversion towards the deep UV. From the spectral point of view the frequency summing process consists of adding the continuous spectrum from the OPG to the comb-like spectrum of the 266 nm radiation (obtained as the fourth-harmonic of a Q-switched Nd:YAG lasers), hence resulting in the required continuous spectrum peaked at 205 nm.

A sketch of the experimental setup that will be assembled is depicted in Fig. 1. Starting from the same pump laser of the infrared OPG–OPA system a beamsplitter conveys about half of the energy to a first frequency doubling stage based on a BBO crystal (BBO1 in Fig. 1) to generate about 75 mJ at a wavelength of 532 nm. A visible beam splitter sends about 3 mJ of the 532 nm pulse to the OPG generating 894 nm radiation, while the remainder is sent to a second frequency doubling stage, based again on a BBO nonlinear crystal (BBO2), which converts the 532 nm pulse into about 15 mJ at 266 nm. The OPG is based on a 30 mm long periodically-poled KTP crystal (PPKTP) which insures an efficiency on the conversion towards 894 nm of about 10 % when pumping with pulses of 3 mJ, hence resulting in pulses of about 300 μJ in the infrared. Finally, the frequency summing stage is composed of a dichroic mirror superposing the radiations at 894 nm and 266 nm, which is followed by a third BBO crystal (BBO3 in Fig. 1) cut to satisfy the type-I phase-matching condition for the process 894 nm + 266 nm → 205 nm, and 3 mm long in order to insure a nonlinear conversion bandwidth larger than 80 GHz for a frequency tuning of the infrared radiation. In the end we expect to obtain about 400 μJ at 205 nm, on a spectrum fulfilling the specifications as discussed above.

In Fig. 2 we report the power generated at 895 nm after the parametric generator (OPG1 following the notation of Fig. 1). The values are in agreement with theoretical expectations and the beam profile shows a regular shape (see the inset in Fig. 2). Concerning the spectral properties of OPG1, in Fig. 3 we show the capability of tuning the wavelength in the region of interest by varying the temperature of the PPKTP crystal, and we characterize the spectral width as a function of the pump energy. While the wavelength-temperature dependence is in good agreement with the theoretical expectations, the spectra of Fig. 3 are about one order of magnitude broader that expected, showing a strong dependence of the spectral width on the pump energy. We attribute this deviation to photorefractive and thermal effects in PPKTP induced by the pump which result in the modulation of the nonlinear crystal properties on the timescale of the pump pulse, and hence a chirp of the parametric process [19]. In Section 3.1 we will present a method to reduce the spectral width of the 895 nm radiation and increase its power spectral density.

Using the spectrum available at the PPKTP output we made a preliminary test of the final frequency summing stage to 205 nm. As mixing medium we use a 3 mm long BBO crystal cut at $\Theta = 59°$ to fulfill the phase-matching condition for the process 895 nm $|o\rangle$ + 266 nm $|o\rangle \leftrightarrow$ 205 nm $|e\rangle$, with both the input and output facets anti-reflection coated at the relevant wavelengths. The fields at 895 nm and 266 nm propagate with an angle of about 4° in order to allow the overlap of the fundamental wavelengths, and the separation of the generated 205 nm without the need of specific dichroic mirrors. As the spectral acceptance of the BBO crystal (0.45 nm at 895 nm, and 0.1 nm at 266 nm) is small compared to the spectral width of the IR field, we expect that only a fraction of the available IR can be converted to 205 nm. Indeed the observed maximum energy converted to 205 nm, (15 ± 2) μJ, is about one order of magnitude less than what expected if there was no limitation arising form spectral acceptance of the BBO and, at the same time, the sensitivity on the alignment of the BBO crystal is less critical that the expected angular acceptance.

3.1. 895 nm spectral filter and amplifier

In order to match the spectrum of the 895 nm field to the requirements on the 205 nm light, we use grating-based spectral selector based on a 1800 lines/mm holographic grating diffracting the IR field at almost grazing incidence. Then, the diffracted beam is imaged on a retro-reflecting mirror partially covered by an iris such that the spectral resolution is 0.85 nm for an aperture of the iris of 1 mm in diameter. As shown in Fig. 4, by changing the aperture of the iris, we are able to select spectral windows in the 900 nm region down to a bandwidth of 1.2 nm, approaching the requirements of our application, and with some margin from further improvements with a more appropriate choice of the IR beam diameter at the position of the diffraction grating. The overall efficiency of the spectral selector is about 50%, mainly limited by the diffraction efficiency of the grating.

In addition to the spectral selector we also tested an amplifier, sketched in Fig. 5, which is based on parametric gain of BBO crystals cut to satisfy the phase-matching for the process 895 nm $|o\rangle$ + 1312 nm $|o\rangle \leftrightarrow$ 532 nm $|e\rangle$. Using two cascaded BBO crystals and pump pulses of 60 mJ we achieved an amplification factor of up to 90. This value, together with the efficiency of the spectral selector, will allow to fulfill both the spectral and energetic requirements on the 895 nm field.

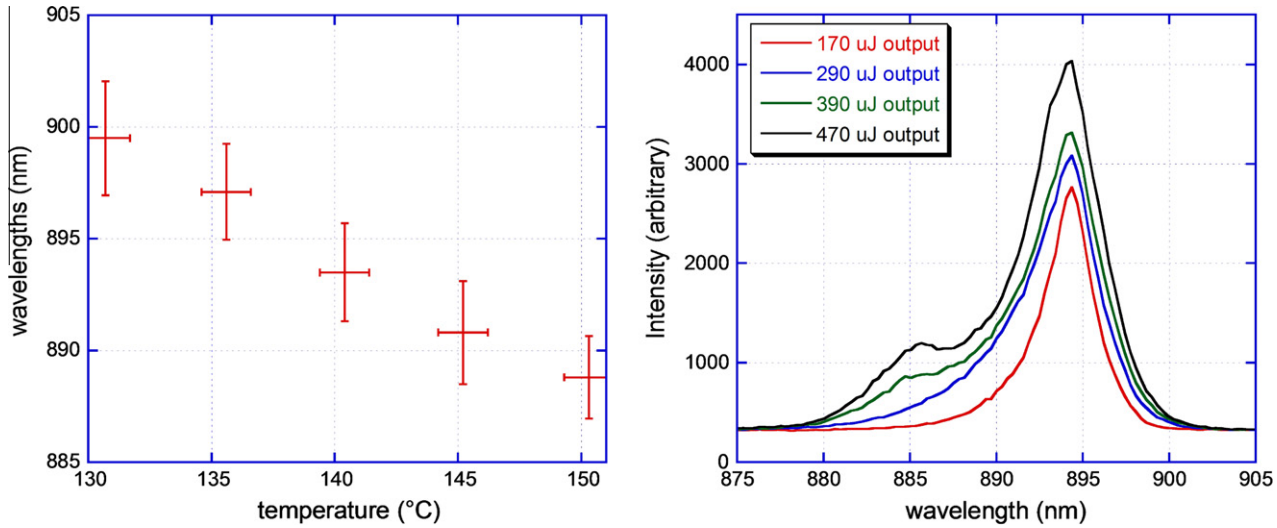

Fig. 3. Left: Variation of the OPG signal wavelength with respect to the PPKTP nonlinear crystal temperature. Stabilizing the PPKTP temperature to better than 1° around 140 °C will allow to reach the resonance condition with the $n = 1 \rightarrow n = 3$ Positronium transition. Right: Spectra of the OPG-generated light at different levels of output energy.

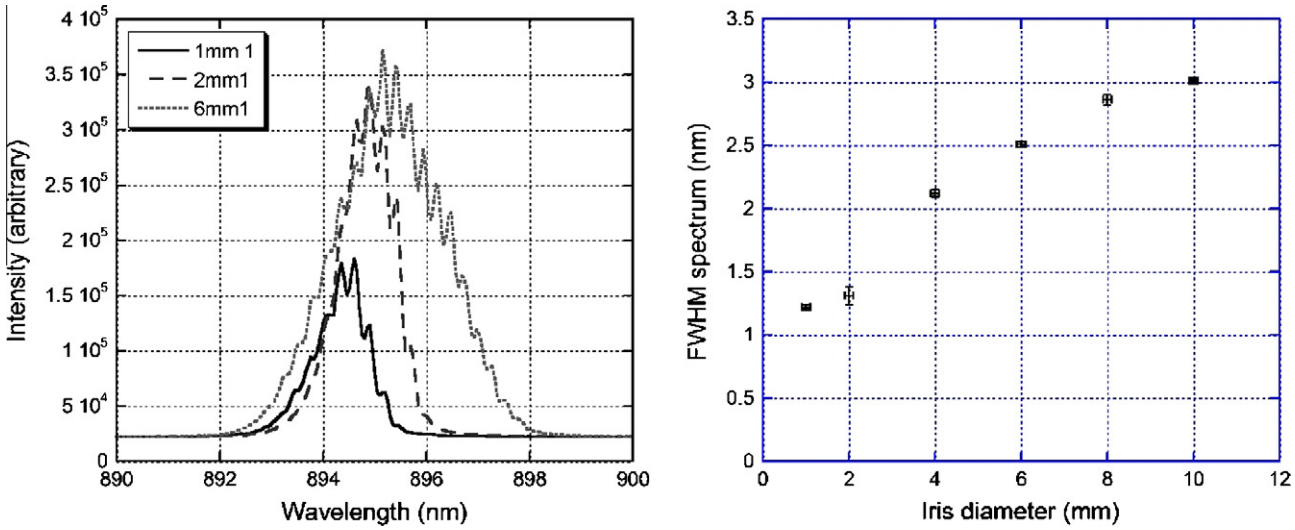

Fig. 4. Operation of the spectral filter. Left: Spectra of the OPG-generated radiation after the filtering stage when varying the aperture of the iris. Right: Spectral width of the filtered radiation VS the iris' aperture.

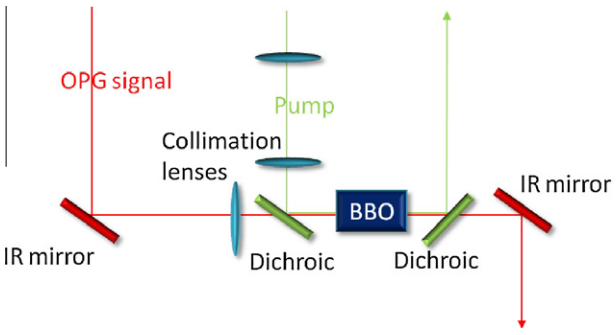

Fig. 5. Sketch of the optical parametric amplifier for the 895 nm light.

4. Conclusions

In this paper we have proposed a new laser system tailored to the task of efficient excitation to Rydberg levels of Ps atoms immersed in a magnetic field, as required by the AEGIS experimental proposal. The system consists of two coupled lasers, one addressed to the $1 \rightarrow 3$ and the other to the $3 \rightarrow n$ transition. Both lasers are based on the technology of parametric generation and amplification, which was chosen because it is appropriate for laser sources with large frequency bandwidth. The laser systems have enough power to guarantee a 30% transition efficiency. The built system can cover a frequency band wide enough to excite different Rydberg levels, while maintaining a great flexibility for the choice of the best strategy for obtaining a large number of antihydrogen atoms.

Acknowledgments

We acknowledge the technical support from D. Cipriani, R. Ballerini and A. Hajeb.

References

[1] A. Kellerbauer et al., Nucl. Instr. Meth. B 266 (2008) 351.
[2] http://doc.cern.ch/archive/electronic/cern/preprints/spsc/public/spsc-2007-017.pdf.

[3] M.G. GiammarchiAEGIS collaboration, Hyperfine Interact. 193 (2009) 321.
[4] E.A. Hessels, D.M. Homan, M.J. Cavagnero, Phys. Rev. A 57 (1998) 1668.
[5] A. Speck, C.H. Storry, E.A. Hessels, G. Gabrielse, Phys. Lett. B 597 (2004) 257.
[6] C.H. Storry et al., Phys. Rev. Lett. 93 (2004) 263401.
[7] F. Castelli, I. Boscolo, S. Cialdi, M.G. Giammarchi, D. Comparat, Phys. Rev. A 78 (2008) 052512.
[8] D.W. Gidley, H.G. Peng, R.S. Vallery, Annu. Rev. Mater. Res. 36 (2006) 49.
[9] S. Mariazzi, P. Bettotti, R.S. Brusa, Phys. Rev. Lett. 104 (2010) 243401.
[10] S.M. Curry, Phys. Rev. A 7 (1973) 447.
[11] C.D. Dermer, J.C. Weisheit, Phys. Rev. A 40 (1989) 5526.
[12] S. Chu, A.P. Mills Jr., Phys. Rev. Lett. 48 (1982) 1333.
[13] K.P. Ziock, C.D. Dermer, R.H. Howell, F. Magnotta, K.M. Jones, J. Phys. B: Atomic Mol. Opt. Phys. 23 (1990) 329.
[14] K.P. Ziock, R.H. Howell, F. Magnotta, R.A. Failor, K.M. Jones, Phys. Rev. Lett. 64 (1990) 2366.
[15] B.W. Shore, K. Bergmann, A. Kuhn, S. Schiemann, J. Oreg, J.H. Eberly, Phys. Rev. A 45 (1992) 5297.
[16] B. Broers, H.B. van Linden van den Heuvell, L.D. Noordam, Phys. Rev. Lett. 69 (1992) 2062.
[17] R.W. Boyd, Nonlinear Optics, second ed., Academic Press, 2003.
[18] A. Borsutzky, R. Brunger, R. Wallenstein, Appl. Phys. B 52 (1991) 380.
[19] U. Bäder, T. Mattern, T. Bauer, J. Bartschke, M. Rahm, A. Borsutzky, R. Wallenstein, Opt. Commun. 217 (2003) 375.